SCIENTIFIC REPORTS

OPEN

SUBJECT AREAS:
NANOBIOTECHNOLOGY
PATHOGENS
PARASITOLOGY
PATHOLOGY

Received
18 June 2012

Accepted
3 August 2012

Published
30 August 2012

Correspondence and requests for materials should be addressed to M.D.-S. (mdiez@mit.edu) or M.D. (mingdao@mit.edu)

* These authors contributed equally to this work.

† Deceased.

Pf155/RESA protein influences the dynamic microcirculatory behavior of ring-stage *Plasmodium falciparum* infected red blood cells

Monica Diez-Silva[1]*, YongKeun Park[2]*, Sha Huang[3], Hansen Bow[3], Odile Mercereau-Puijalon[4], Guillaume Deplaine[4], Catherine Lavazec[4], Sylvie Perrot[4], Serge Bonnefoy[4], Michael S. Feld[5†], Jongyoon Han[3], Ming Dao[1] & Subra Suresh[1]

[1]Department of Materials Science and Engineering, Massachusetts Institute of Technology, Cambridge, MA 02139, USA, [2]Department of Physics, Korea Advanced Institute of Science and Technology, Daejeon 305-701, Republic of Korea, [3]Department of Electrical Engineering and Computer Science, Massachusetts Institute of Technology, Cambridge, MA 02139, USA, [4]Unité d'Immunologie Moléculaire des Parasites, CNRS URA 2581, Département de Parasitologie/Mycologie, Institut Pasteur, 28 rue du Dr. Roux, 75734 Paris Cedex 15, France, [5]G. R. Harrison Spectroscopy Laboratory, Massachusetts Institute of Technology, Cambridge, Massachusetts 02139, USA.

Proteins exported by *Plasmodium falciparum* to the red blood cell (RBC) membrane modify the structural properties of the parasitized RBC (*Pf*-RBC). Although quasi-static single cell assays show reduced ring-stage *Pf*-RBCs deformability, the parameters influencing their microcirculatory behavior remain unexplored. Here, we study the dynamic properties of ring-stage *Pf*-RBCs and the role of the parasite protein *Pf*155/Ring-Infected Erythrocyte Surface Antigen (RESA). Diffraction phase microscopy revealed RESA-driven decreased *Pf*-RBCs membrane fluctuations. Microfluidic experiments showed a RESA-dependent reduction in the *Pf*-RBCs transit velocity, which was potentiated at febrile temperature. In a microspheres filtration system, incubation at febrile temperature impaired traversal of RESA-expressing *Pf*-RBCs. These results show that RESA influences ring-stage *Pf*-RBCs microcirculation, an effect that is fever-enhanced. This is the first identification of a parasite factor influencing the dynamic circulation of young asexual *Pf*-RBCs in physiologically relevant conditions, offering novel possibilities for interventions to reduce parasite survival and pathogenesis in its human host.

Shortly after invasion of the red blood cell (RBC), the malaria parasite *Plasmodium falciparum* initiates a profound remodeling of its host cell by delivering proteins to the RBC membrane[1]. As the parasite matures, the membrane properties of *P. falciparum* infected-RBCs (*Pf*-RBCs) are modified, with markedly decreased cell deformability and acquired cytoadherence properties[2–5]. Altogether, these modifications affect the dynamic behavior of *Pf*-RBCs altering blood flow and contributing to malaria pathophysiology[6].

Pf-RBCs *dynamic* properties are critical at the ring-stage of the infection, since this is the only asexual intra-erythrocytic stage in the peripheral circulation. Both microcapillary circuits and splenic red pulp sinus slits dynamically challenge the mechanical properties of *Pf*-RBCs. Several single cell assays have documented a moderate decrease in deformability of ring-stage *Pf*-RBCs[4,7]. Furthermore, there occurs a decrease in membrane flickering of *Pf*-RBCs starting at the ring stage of the infection[8]. Its consequences for the dynamic microcirculatory behavior of ring-stage *Pf*-RBCs are unclear. How deformability measures of *Pf*-RBCs assayed in static conditions translate in alteration of the microcirculatory behavior remains an open question.

In the present study, we use different approaches to document the *dynamic* properties and the *circulatory* behavior of *Pf*-RBCs at the ring-stage of the infection and explore the contribution of the parasite-encoded *Pf*155/Ring-Infected Erythrocyte Surface Antigen (RESA), which has been identified as a major contributor to the reduced ring-stage *Pf*-RBCs deformability in static conditions[9]. RESA is located in the dense granules of the invasive merozoites[10], released shortly after invasion into the parasitophorous vacuole[11] and rapidly translocated to the internal face of the *Pf*-RBC membrane. RESA is then phosphorylated[12] and remains associated with spectrin[13] for the first 24 h of the asexual intra-erythrocytic development. The binding site of RESA to spectrin

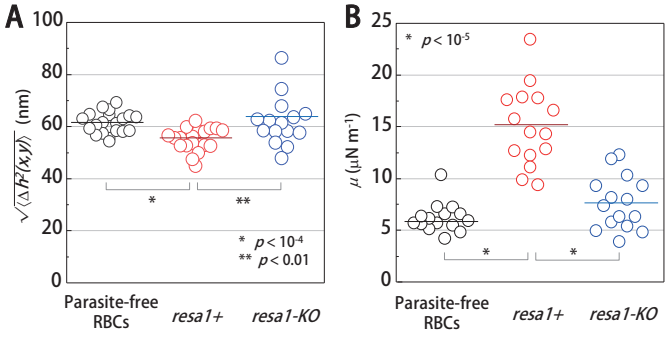

Figure 1 | Membrane dynamics of ring-stage *Pf*-RBCs at physiological body temperature. (A) RMS displacements, and (B) in-plane shear modulus values of parasite-free RBC, wild-type *resa1*+ and *resa1-KO* ring-stage *Pf*-RBCs. Open circles are experimental values and represent individual cell measurements. Significant differences are shown as * ($p < 10^{-4}$) and * ($p < 10^{-5}$) values.

has been localized to repeat 16 of the β-chain[14]. This interaction appears to favor the tetrameric spectrin state, resulting in membrane mechanical stabilization and increased membrane thermal stability[14]. As a result, RESA protects *Pf*-RBCs from vesiculation damage induced at high temperature[14–16]. Our earlier work under *static* conditions revealed that the role played by RESA decreasing the deformability of *Pf*-RBCs at the ring stage of the infection was dramatically enhanced at febrile temperature[9]. Here we use wild-type *resa1*+, *resa1*− and resa1-rev (the revertant isogenic *resa1*-rev *Pf*-RBCs) genetically modified parasites[9] to analyze the dynamic properties of ring-stage *Pf*-RBCs. The resa1-rev was constructed specifically to confirm targeted gene disruption. Since no differences in membrane stiffness between wild-type *resa1*+ and resa1-rev were observed[9] either resa1+ wild type or resa1+ revertant are used in this study as a control condition. We analyze, by diffraction phase microscopy (DPM)[17,18], the membrane dynamics of ring-stage *Pf*-RBCs at physiological normal and febrile temperature. To assess the physiological implication of decreased deformability of ring-stage *Pf*-RBCs in microcirculation, we used microfluidic technology with multiple constrictions[19] that replicate *in vitro* the mechanical challenges imposed to *Pf*-RBCs *in vivo*. We document in real-time the ultimate impact of RESA protein on *Pf*-RBCs dynamic response, quantitatively comparing transit cell velocities of individual *Pf*-RBCs, expressing or not expressing RESA, as they are forced to traverse successive constrictions under controlled pressure gradients. Moreover we study the effects of febrile temperature and expression of RESA on the circulatory behavior of ring-stage *Pf*-RBCs through a microspheres microsphiltration system[20], shown to mimic the mechanical challenge of *Pf*-RBCs by the human spleen by imitating the geometry of narrow and short inter-endothelial slits of the spleen sinuses.

Results

Decreased membrane dynamics in ring-stage *Pf*-RBCs are RESA-driven. We first addressed the effect of RESA on membrane dynamics of ring-stage *Pf*-RBCs using Diffraction Phase Microscopy (DPM). RBC samples were prepared under three different conditions: parasite-free RBCs, wild-type *resa1*+ and *resa1*-KO ring-stage *Pf*-RBCs (see *Materials and Methods*). In order to compare the dynamic membrane fluctuations of the different types of RBC samples, we calculated the root mean square (RMS) displacement of membrane fluctuation, $\sqrt{\langle \Delta h^2 \rangle}$, which covers the entire cell area for 2 s at 120 frames/s (Figure 1A). The RMS displacement of membrane fluctuations for parasite-free RBCs was 61 ± 4.0 nm. Membrane fluctuations decreased significantly to 55.0 ± 4.3 nm in wild-type *resa1*+ *Pf*-RBCs. However, membrane fluctuations in *resa1*-KO *Pf*-RBCs showed higher values than wild-type *resa1*+ *Pf*-RBCs (62.0 ± 9.0 nm). No significant difference between membrane fluctuations in *resa1*-KO *Pf*-RBCs and parasite-free RBCs was observed.

We then retrieved the in-plane shear modulus μ, which determines the ability of RBCs to deform. The results for the shear modulus are shown in Figure 1B. For parasite-free RBCs, $\mu = 6.2 \pm 1.4$ μN/m. A significant increase in μ was observed for wild-type *resa1*+ *Pf*-RBCs (15.0 ± 3.8 μN/m), indicating a decrease in cell deformability. Interestingly a significant decrease in μ is observed for *resa1*-KO *Pf*-RBCs (7.6 ± 2.6 μN/m). These results are consistent with literature values of membrane shear modulus obtained using independent

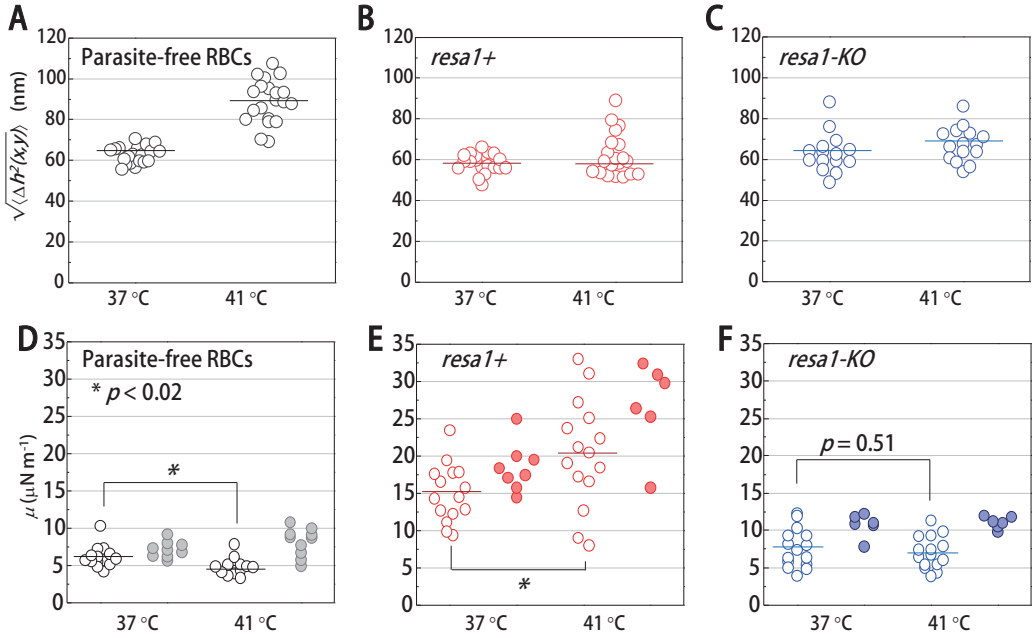

Figure 2 | Membrane fluctuations and in-plane shear modulus of ring-stage *Pf*-RBCs at body and febrile temperature. RMS displacement histogram and in-plane shear modulus values (upper and lower panel, respectively) of (A), (D). parasite-free RBCs, (B), (E). *resa1*+, and (C), (F). *resa1-KO* ring-stage *Pf*-RBCs, measured at 37°C and 41°C. Open circles represent individual RBC measurements. Closed circles are shear modulus results obtained with optical tweezers and the same set of parasites[9] shown for comparaison purposes. Significant differences are shown as * ($p < 0.02$) values.

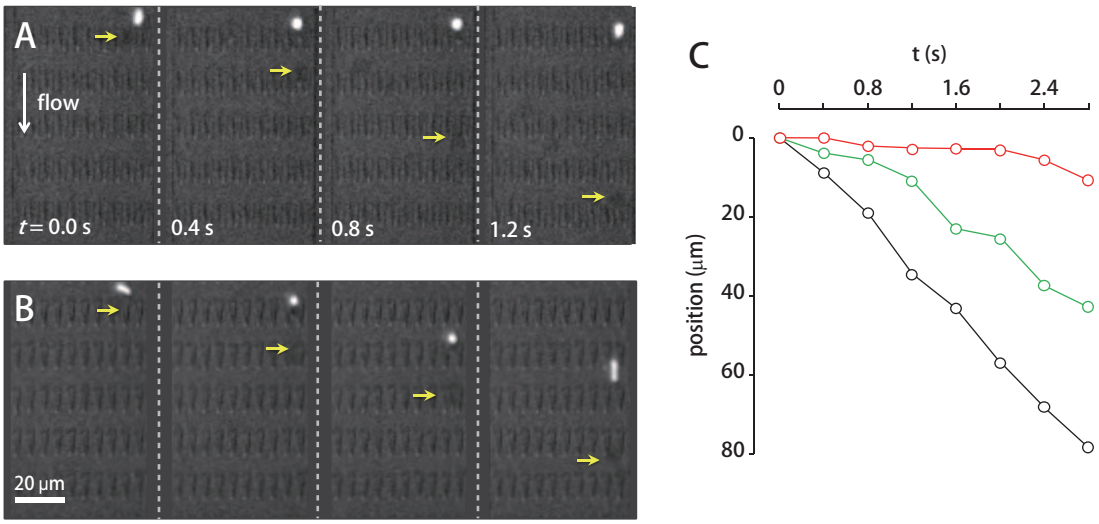

Figure 3 | Differences in the dynamic response of ring-stage *Pf*-RBCs expressing or not RESA. Real-time snap-shots transit cell velocity of a representative example of all the experiments performed of (A) *resa1*+, and (B) *resa1*-KO ring-stage *Pf*-RBCs, forced to traverse through 3 µm successive constrictions in micro-sized channels at a constant pressure gradient of 0.24 Pa µm^{-1}. *Pf*-RBCs are labelled fluorescently using Thiazole orange. Yellow arrows indicate individual parasite-free RBC. (C). Illustrative example of all the transit cell velocity measurements performed. Each open circle represents the spatial position (µm) as a function of time (s) of individual *resa1*+ (red) and *resa1*-KO (green) *Pf*-RBCs compared to parasite-free RBCs (grey) calculated from Figure 3A and B.

experimental methods under static conditions that involved optical tweezers tests on parasite-free RBCs[6,7], wild-type *resa1*+ and *resa1*-KO ring-stage *Pf*-RBCs[9], and previous work on 3D7 ring-stage wild-type *Pf*-RBCs using DPM measurements[8].

Temperature enhances membrane dynamics of ring-stage *Pf*-RBCs. Membrane fluctuation values derived from the DPM measurements susbtantially increased from normal physiological to febrile temperature in parasite-free RBCs (Figure 2A), while the in-plane shear modulus values decreased (Figure 2D). In contrast, membrane fluctuations of *resa1*+ *Pf*-RBCs were essentially similar at 37°C and 41°C (Figure 2B), but the in-plane shear modulus showed a significant decrease in cell deformability from body to febrile temperature, although the scatter range was large (Figure 2E). *Resa1*-KO *Pf*-RBCs DPM measurements showed that membrane fluctuations values were somewhat higher at 41°C than those observed at 37°C (Figure 2C), although the increase was modest compared to parasite-free RBCs. The *resa1*-KO *Pf*-RBCs in-plane shear modulus showed no significant difference between normal and febrile temperature as observed for parasite-free RBCs (Figure 2F). Results on membrane shear modulus measurements obtained previously using optical tweezers test on parasite-free RBCs, wild-type *resa1*+ and *resa1*-KO ring-stage *Pf*-RBCs[9] are shown for comparison (closed circles Figure 2 D–F).

Microcirculation of ring-stage *Pf*-RBCs is influenced by RESA. The effect of RESA expression on the dynamic properties of ring-stage *Pf*-RBCs was measured using a microfluidic assay quantifying the transit cell velocity of *Pf*-RBCs moving through channels with multiple successive constrictions under controlled pressure, and thereby simulating host microcirculation *in vitro*. Figure 3 shows in real time a representative example of the dynamic response of parasite-free RBCs, *resa1*+ and *resa1*-KO ring-stage *Pf*-RBCs when they were forced to pass through multiple constrictions at normal physiological (37°C) temperature. At a constant gradient pressure of 0.24 Pa µm^{-1} ring-stage *Pf*-RBCs were able to deform and squeeze through micro-sized constrictions of 3 µm. However, when compared to the transit cell velocity of parasite-free RBCs

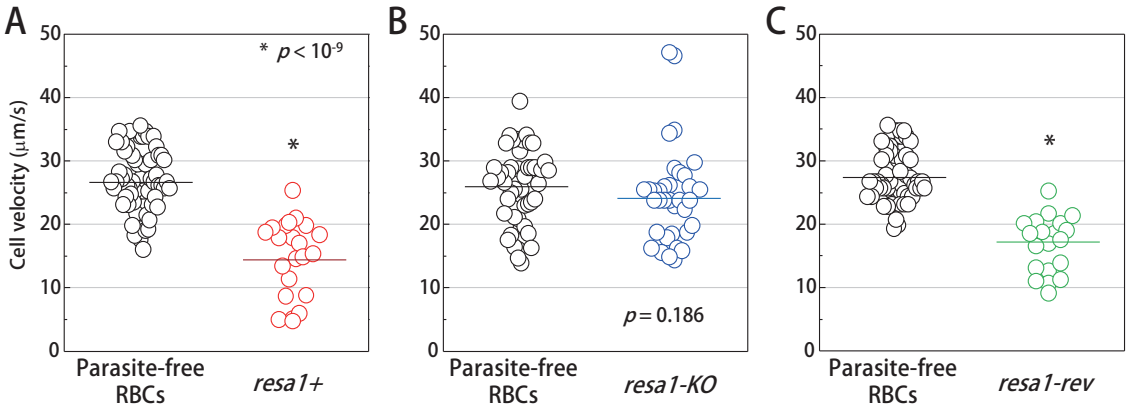

Figure 4 | Transit cell velocity of ring-stage *Pf*-RBCs at body temperature. Transit cell velocities of (A) *resa1*+, (B) *resa1*-KO and (C) *resa1*-rev ring-stage *Pf*-RBCs compared to corresponding co-cultured parasite-free RBCs, passing through 3 µm constrictions in micro-sized channels. Measurements were performed at 37°C at a constant pressure gradient of 0.24 Pa µm^{-1}. Each open circle represents an individual cell measurement. Significant differences are shown as * ($p < 10^{-9}$) values.

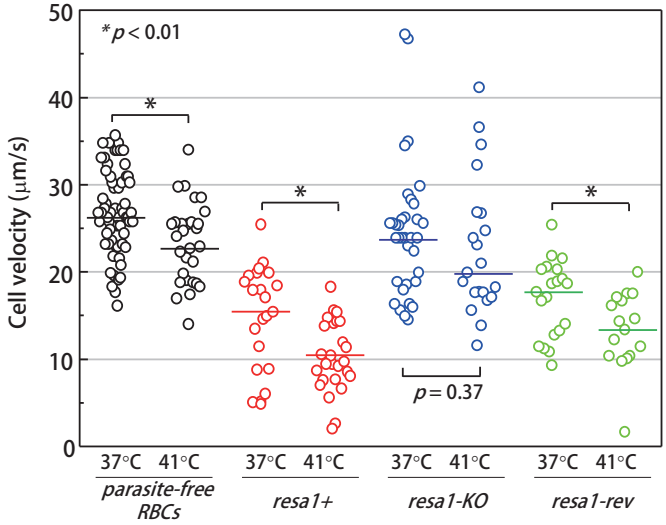

Figure 5 | Transit cell velocity of ring-stage *Pf*-RBCs at body and febrile temperature. Transit cell velocities of parasite-free RBCs (black), *resa1*+ (red), *resa1*-KO (blue) and *resa1*-rev (green) ring-stage *Pf*-RBCs, measured at 37°C and 41°C. Measurements were performed at a constant pressure gradient of 0.24 Pa μm^{-1}. Each open circle represents an individual cell measurement. Significant differences are shown as * ($p < 0.01$) values.

appearing in each field of view, the transit cell velocity of individual *resa1*+ *Pf*-RBCs (Figure 3A and supplementary material Video S1) was significantly slower than *resa1*-KO ring-stage *Pf*-RBCs (Figure 3B and supplementary material Video S2). As an illustrative example of all the cell velocity measurements performed, the spatial position as a function of time of individual *resa1*+ and *resa1*-KO *Pf*-RBCs compared to parasite-free RBCs (calculated from Figure 3A and B) are represented in Figure 3C. The average transit cell velocity of *resa1*+ *Pf*-RBCs (14.7 μm/s) was slower than parasite-free RBCs from the same culture (26.8 μm/s, $p < 0.001$) (Figure 4A). However, *resa1*-KO *Pf*-RBCs and bystander parasite-free RBCs exhibited similar transit cell velocities (24.5 and 25.9 μm/s, respectively, with $p = 0.186$) (Figure 4B).

To further substantiate that the observed difference in transit cell velocity between *resa1*-KO *Pf*-RBCs and *resa1*+ *Pf*-RBCs was specifically due to the absence of RESA protein expression, we tested the dynamic response of the revertant isogenic *resa1*-rev *Pf*-RBCs[9]. The *resa1*-rev *Pf*-RBCs displayed markedly decreased average transit cell velocity (16.8 μm/s) in the same range as the original *resa1*+ parental line, and substantially lower than bystander parasite-free RBCs (28.1 μm/s) ($p < 0.001$) (Figure 4C).

The effect of RESA on *Pf*-RBCs microcirculation *in vitro* was also investigated at febrile temperature. Indeed, the transit cell velocity of wild-type *resa1*+ *Pf*-RBCs was reduced (Figure 5A) when microfluidics experiments were performed at 41°C (10.2 μm/s compared to 14.7 μm/s at 37°C, $p < 0.01$). *Resa1*-rev *Pf*-RBCs behaved similarly, with an average transit cell velocity of 13.2 μm/s at 41°C and 16.8 μm/s at 37°C ($p < 0.01$) (Figure 5C). However *resa1*-KO *Pf*-RBCs, which had similar transit cell velocity values at both 37°C and 41°C (24.5 μm/s and 22.6 μm/s, respectively, $p=0.1863$) displayed a similar trend as the parasite-free RBCs from 37°C to 41°C (26.8 μm/s and 23.30 μm/s $p < 0.01$) (Figure 5B).

Temperature and RESA expression influence filterability of ring-stage *Pf*-RBC in microspheres. The effect of RESA on the circulatory behavior of ring-stage *Pf*-RBCs was assessed using microspheres, a microspheres filtration system simulating the narrow and short geometry of inter-endothelial slits of the spleen sinuses[20]. Highly synchronized cultures (ring stage at 15-18 h) pre-incubated for 3 h at 37°C or 40°C were loaded on the calibrated microspheres columns. Traversal of *Pf*-RBCs was quantified by calculating the retention rate in the microspheres. Retention of *resa1*-KO and *resa1*-rev *Pf*-RBCs did not differ significantly in the culture maintained at 37°C (Figure 6A). However, it was increased by 30-60% in *resa1*-rev *Pf*-RBCs pre-incubated for 3 h at 40°C and not in *resa1*-KO *Pf*-RBCs (Figure 6A). To rule out that increased retention of *resa1*-rev parasites was due to a more advanced parasite developmental stage, possibly more rapid development during the 3 h exposure at 40°C, the duration of the temperature shift was reduced to 2 h and synchronous parasites at different stage of development were used. Temperature-shifted 12–15 h old or 15–18 h old *resa1*-rev ring stage *Pf*-RBCs displayed a higher retention rate compared to the sibling culture maintained at 37°C. Such a temperature-induced reduced filterability was not observed for the

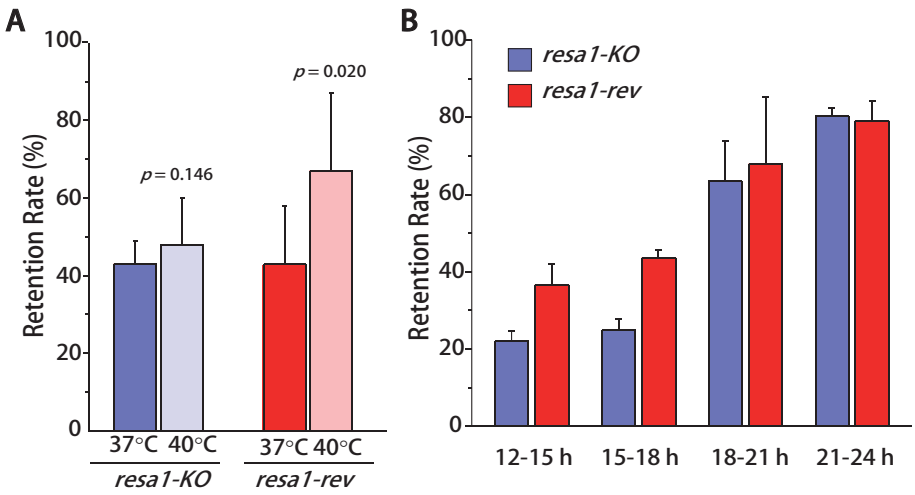

Figure 6 | Incubation at febrile temperature increases retention rate by microspheres of RESA expressing *Pf*-RBCs (*resa1*-rev) and not of *resa1*-KO ring-stage *Pf*-RBCs. (A) Synchronized cultures (15–18 h rings) of *resa1*-rev (red) and *resa1*-KO (blue) *Pf*-RBCs adjusted to 2% hematocrit and 10% parasitemia, were incubated at either at 37°C or 40°C for 3 h. Error bars represent the standard deviation. (B) Highly synchronized parasite cultures (12–15 h, 15–18 h, 18–21 h and 21–24 h after invasion) of *resa1*-rev (red) and *resa1*-KO (blue) *Pf*-RBCs adjusted to 2% hematocrit and 5% parasitemia, were incubated at 40°C for 2 h. Error bars represent the standard deviation. The *p* values for *resa1*-rev/*resa1*-KO are 0.07 for 12–15 h; 0.00066 for 15–18 h; 0.397 for 18–21 h, and 0.641 for 21–24 h.

resa1-KO *Pf*-RBCs cultures (Figure 6B). This indicated that RESA expression influenced microsphere filterability of fever-exposed ring-stages. At a later developmental stage, as anticipated, filterability was further reduced and was RESA-independent, as *Pf*-RBCs harbored mature, poorly deformable parasites.

Discussion

The results presented here demonstrate that expression of RESA protein in the ring stage of intra-erythrocytic development of *P. falciparum* has a significant effect on dynamic biophysical properties and microcirculatory response of *Pf*-RBCs. They also provide clear evidence that ring-stage *Pf*-RBCs markedly differ in their microcirculatory behavior from bystander parasite-free RBCs and from ring-stage *Pf*-RBCs devoid of RESA. Febrile temperature exacerbates the role of RESA in influencing the dynamic microcirculatory properties of *Pf*-RBCs.

Nanoscale fluctuations (commonly referred to as "flickering") of the cell membrane at 37°C are markedly decreased by RESA expression in the ring stage. This is consistent with a reported reduction in thermally driven membrane flickering over the full range of (wild-type) infected stages of *Pf*-RBCs[8]. It had been speculated that parasite modifications to the host RBC cytoskeleton are responsible for changes in the *Pf*-RBCs membrane flickering profile. The membrane fluctuation values at 37°C on *resa1*-KO *Pf*-RBCs and parasite-free RBCs were comparable, indicating that the presence of RESA on host membrane, or downstream effects of its expression, are involved in the membrane flickering changes observed in young stages at normal body temperature. The in-plane shear modulus data retrieved from the measured membrane fluctuations values indicate increased rigidity for the *Pf*-RBCs expressing RESA but not for *resa1*-KO *Pf*-RBCs. These results are in agreement with optical tweezers measurements of quasi-static deformation[9], and confirm that RESA protein modulates cell deformability of ring-stage *Pf*-RBCs.

We found febrile temperature to significantly influence the membrane dynamic properties of parasite-free RBCs present in the same culture as ring-stage *Pf*-RBCs. The membrane fluctuation of parasite-free RBCs increased from normal physiological (37°C) to febrile (41°C) temperature while the in-plane shear modulus decreased. This latter observation is in line with the reported decrease by ≈ 20% of the shear modulus of healthy RBC membrane when the temperature increased from 23 to 41°C[21]. This indicates an increase in the overall parasite-free RBCs deformability at febrile temperature, possibly reflecting structural changes of the RBC membrane phospholipid and/or spectrin network that alter its elastic properties[8]. One possible contributor is the transitional structural change in α- and β-spectrin molecules near 40°C[22]. Interestingly, different observations were made with ring-stage *resa1*+ *Pf*-RBCs. Since the in-plane shear modulus of RBCs in our results is calculated from the tangential component of displacement in membrane fluctuations[23], both the measured axial membrane fluctuation and morphology of RBCs determined shear modulus value. No significant changes in membrane fluctuations were observed upon temperature shift in *resa1*+ *Pf*-RBCs while the in-plane shear modulus values increased, i.e. both parameters showed opposite trends compared to bystander parasite-free RBCs. Since RESA interaction with spectrin stabilizes spectrin's tetrameric state *in vitro*[14], it probably prevents the dissociation of spectrin tetramers at 41°C, resulting in overall decreased *Pf*-RBCs deformability and increased membrane mechanical stability[14]. This inference is also consistent with the earlier finding that RESA prevents membrane vesiculation at 50°C[15,16]. The RESA-dependent temperature enhancement of ring-stage *Pf*-RBCs stiffness observed here is consistent with previous static deformability measurements obtained using optical tweezers[9]. At 41°C, a modest increase in membrane fluctuations was recorded in *resa1*-KO *Pf*-RBCs compared to that observed at 37°C. This indicates that in addition to RESA expression, possibly other parasite-associated factors contribute to modulating ring-stage *Pf*-RBCs membrane fluctuations at 41°C. Possible parasite factors influencing membrane fluctuations changes at 41°C are additional parasite-encoded proteins and/or apical organelle-associated proteins discharged in the erythrocyte-membrane during invasion[24–26]. Alternative RESA-independent modifications are proteolysis of band3 and/or of erythrocyte cytoskeletal proteins needed to ensure invasion[27–29]. Although *Pf*-RBCs lacking RESA showed increased membrane fluctuations values at 41°C, the in-plane shear modulus remained essentially unaffected at 37°C and 41°C. The data confirm RESA as the main molecule involved in *Pf*-RBCs deformability changes observed at elevated temperature, and support the role played by the specific RESA-spectrin interaction at 41°C.

Analysis of the dynamic properties of *Pf*-RBCs using a microfluidic device that replicates successive constriction obstacles encountered in the vascular microcirculation was done at physiological and febrile temperatures. Transit cell velocity of ring-stage *resa1*+ *Pf*-RBCs was markedly decreased compared to bystander parasite-free RBCs, and was further reduced at febrile temperature. Although *resa1*-KO *Pf*-RBCs travelled slightly slower than the co-cultured parasite-free RBCs, this was not statistically significant, and moreover transit cell velocity was independent of the temperature at which the experiments were performed. The similarly higher transit cell velocities of *resa1*-KO *Pf*-RBCs and parasite-free RBCs indicate that RESA is largely responsible for the reduced transit cell velocity of ring-stage *Pf*-RBCs. This data identifies for the first time RESA as a parasite factor is able to modulate the dynamic response of ring-stage *Pf*-RBCs during microcirculation.

In addition to vascular microcirculation, another anatomical site where RBC dynamic properties are stringently challenged is the red pulp of the human spleen where the RBCs must undergo extensive deformation as they cross the narrow inter-endothelial slits of the sinuses. In an *ex vivo* organ perfusion system, a significant proportion of ring-stage *Pf*-RBCs was retained in the red pulp of the human spleen, most probably due to their altered mechanical properties[30]. The bead microsphiltration system we used here mimics the mechanical sensing of RBCs by the human spleen, as it was shown to retain ring-stage *Pf*-RBCs at a rate similar to that observed in an isolated-perfused human spleen[20]. This system does not permit assessment of the behavior of bystander parasite-free RBCs, but allows us to monitor the filterability of *Pf*-RBCs and hence the impact of the presence of RESA and of a temperature shift on efficiency of traversal of the microsphere layer. Filterability of *resa1*-rev and r*esa1*-KO *Pf*-RBCs was similar at 37°C, but a transient incubation at 40°C resulted in increased retention of the RESA expressing *Pf*-RBCs and not of the r*esa1*-KO *Pf*-RBCs. Such a temperature-associated decreased filterability of RESA-expressing parasites was observed for late ring-stage Pf-RBCs, and was not observed in mature stages, which no longer express RESA. The late ring stage parasites studied here were harvested before surface expression of the *P. falciparum* erythrocyte membrane protein 1 (*Pf*EMP1)[31]. Furthermore no difference in retention with the bead system could be observed over the first 20 hours post invasion between K+ or K− parasites[32] excluding a possible effect of knobs in bead retention. Thus, the microsphiltration results show that RESA expression clearly modulates the circulatory behavior of *Pf*-RBCs at febrile temperature.

Our data present the first detailed evidence for a major role of temperature and presence of RESA in modulating the dynamic microcirculation characteristics of ring-stage *Pf*-RBCs. This conclusion, stemming from the analysis of dynamic behavior of *Pf*-RBCs using complementary approaches that impose distinct geometric constraints on dynamic cell deformabilty, is consistent with observations of the static behavior of ring *Pf*-RBCs, using optical tweezers[9] and biophysical measurements[4,7]. The consistency of data obtained on the static and dynamic behaviour on the one hand and biophysical measurements on the other is interesting as it cross-validates the

various, complementary approaches. Moreover, data presented here as well as previous studies[4,7–9] point to RESA as a major determinant of the temperature-enhanced deformability defect of ring-stage *Pf*-RBCs.

RESA may play a bifunctional role on influencing microcirculation of ring-stage *Pf*-RBCs during an *in vivo* infection. While its expression is essential for the young ring stage parasites to resist a transient exposure to febrile temperature and ensure their normal intra-erythrocytic cycle and parasite development[9], upon exposure of febrile temperatures can possibly lead to a splenic retention and accelerated parasite clearance.

The present findings open new avenues for intervention to reduce parasite survival and pathogenesis in its human host.

Methods

Parasites and culture. The *P. falciparum* FUP/CB line (referred to as wild-type *resa1*+) and its derived *resa*1 gene knock-out *P. falciparum* clone (*resa1*-KO) and *resa1*-revertant clone (*resa1*-rev)[9] were cultured in leukocyte-free human RBCs (Research Blood Components, Brighton, MA) under an atmosphere of 5% O_2, 5% CO_2 and 95% N_2, at 5% haematocrit in RPMI culture medium 1640 (Gibco Life Technologies, Rockville, MD) supplemented with 25 mM HEPES (Sigma), 200 mM Hypoxanthine (Sigma, St. Louis, MO), 0.20% NaHCO3 (Sigma, St. Louis, MO) and 0.25% Albumax I (Gibco Life Technologies, Rockville, MD). Parasite cultures were routinely synchronized in ring stage by using Sorbitol lysis 2 h after merozoite invasion[33]. Prior to measurements the parasite cultures were enriched in late trophozoite stages at 96% purity using a Midi MACS LS magnetic column (Miltenyi Biotech, Auburn, CA) and diluted into RBCs obtained the same day, to harvest in the next cycle highly synchronous ring stages in fresh RBCs.

Diffraction phase microscopy. RBCs and *Pf*-RBCs samples were centrifuged at 125 *g* and diluted in Phosphate buffered saline (PBS), 1% Bovine Serum Albumin (BSA) (Sigma-Aldrich, St Louis, MO) to approximately 1×10^6 RBCs/mL. A 10 μL RBC suspension was introduced between two glass slides and the dynamic membrane fluctuations were measured using Diffraction Phase Microscopy (DPM)[8]. DPM is a highly stable and sensitive quantitative phase microscopy, which employs the laser interferometry in a common path geometry and thus provides full-field quantitative phase images of biological samples with unprecedented optical path length stability[17,18]. An Ar^{2+} laser (λ=514 nm, Coherent Inc., Santa Clara, CA) was used as illumination source. An inverted microscope (IX71, Olympus American Inc., Center Valley, PA) was equipped with a 40x objective (0.65 NA), which facilitates a diffraction-limited transverse resolution of 400 nm. With the additional relay optics, the overall magnification of the system was 200×. EMCCD (Photonmax512B, Princeton Instruments, Trenton, NJ) was used to record interferograms. The instantaneous cell thickness map is obtained as $h(x,y,t) = \lambda/(2\pi\Delta n)\cdot\phi(x,y,t)$, with ϕ the quantitative phase image measured by DPM. The refractive index contrast Δn between the RBC and the surrounding medium is mainly attributed to hemoglobin in RBC cytosol. The values for Δn were used from a previous study[8]. The DPM optical path length stability is 2.4 mrad, which corresponds to a membrane displacement of 3.3 nm in RBC membrane[18].

By retrieving the optical path length shifts produced across the cell, the cell thickness profiles at a given time *t, h(x,y,t),* were obtained. The dynamic membrane fluctuation can then be calculated by subtracting the averaged cell shape from the instantaneous cell thickness map, $\Delta h(x,y,t) = h(x,y,t) - \langle h(x,y)\rangle$, where the brackets represent the average over time.

The in-plane shear modulus of the RBC membrane, μ, can be retrieved from the measured membrane fluctuations[8]. We calculated μ by using Fourier-transformed Hamiltonian (strain energy) and equi-partition theorem[23]:

$$\mu \approx \frac{k_B T \ln(A/a)}{3\pi\langle \Delta h_t^2 \rangle}$$

Where A is the diameter of RBC, and a is the minimum spatial wavelength measured by DPM (400 nm). The tangential component of displacement in membrane fluctuations Δh_t^2 was decoupled from the measured axial membrane fluctuations Δh_t^2 and the normal diffraction of the membrane, which can be calculated from the mean cellular thickness map measured by DPM[8].

The microscopic set up was equipped with a temperature controller (TC-202A, Warner Instruments, Hamden, CT), which uses a thermistor to set the temperature of the sample to within ±0.2°C. The well containing RBCs was placed in contact with the controller chamber, and heat transfer and thermal equilibrium between the two systems were attained relatively fast, after 3–4 min. We measured the individual RBC response at different temperature points after a ~10 min incubation for each new temperature to ensure thermal equilibrium. DPM measurements were performed at 37°C and 41°C, on ring-stage parasites (14–18 h post-invasion).

Microfluidic channel fabrication. A microfluidic device was made of polydimethylsiloxane (PDMS) using photolithography and reactive-ion etching (RIE) techniques as described elsewhere[19]. The microfluidic device pattern was designed specifically for the capillary channels to test optimum RBC deformation. Briefly, the microfluidic device consisted of multiple parallel capillary channels with triangular pillars arrays, producing successive micro-sized constrictions of 3.0 μm between pillars, with a depth of 4.2 μm[19]. The inlet and the outlet reservoir have the same dimensions of 500 x 500 μm^2.

Microfluidic measurements. RBCs and *Pf*-RBCs were centrifuged at 300 *g*, and further diluted in PBS-1% BSA to a 0.5% hematocrit. Thiazole orange (0.05 μM) (Invitrogen, Carlsbad, CA) was added to the suspension and samples were incubated at room temperature for 20 min in the dark. Then, a 10 μL RBCs suspension was flowed through the microfluidic device previously coated with PBS-1%BSA, at a constant pressure gradient of 0.24 Pa μm^{-1} [19]. All experiments were imaged using an inverted fluorescent microscope (Olympus IX71, Center Valley, PA) equipped with a 60x objective and connected to a CCD camera (Hamamatsu Photonics, C4742-80-12AG, Japan). Images of individual RBC were acquired automatically using IPLab (Scanalytics, Rockville, MD) at 70 ms time interval using a green illumination (545 nm). Post-imaging analysis was done using imageJ software (National Institutes of Health).

The temperature was controlled using a heating chamber (Olympus, Center Valley, PA), which was preheated 30 min before the beginning of the experiment. Then a PBS-1%BSA coated microfluidic device was placed into the heating chamber 5 min before loading the RBCs suspension. A thermal meter was used to probe the exact temperature inside the heating chamber and 5 min were required for the temperature to be adjusted to a different value.

Transit cell velocities of individual RBCs and *Pf*-RBCs passing through microchannels were analyzed. Microfluidic measurements were performed at 37°C and 41°C, on ring stage-parasites (14–18 h post invasion).

Microsphiltration. Microspheres sphiltration was performed using methods previously established[20]. Briefly, 2 g of dry calibrated metal microspheres (96.50% tin, 3.00% silver, and 0.50% copper; Industrie des Poudres Sphériques, France) with 2 different size distributions (5- to 15-μm-diameter and 15- to 25-μm-diameter) were mixed and then suspended in 8 mL of RPMI 1640/10% human serum. Nine hundred μL of the bead suspension was poured into an inverted 1000 μL anti-aerosol pipette tip (Neptune, BarrierTips) and allowed to settle, leading to the formation of a 5 mm-thick bead layer above the anti-aerosol filter. 600 μL of a 2% hematocrit RBC suspension containing less than 10% of potentially "retainable" RBC (to avoid bead saturation) was introduced upstream from the micro-bead layer. RBCs were flushed through the bead layer at a flow rate of 60 mL/h using an electric pump (Syramed μsp6000, ARCOMED AG, Regensdorf, Switzerland). The bead layer was then washed with 6 mL RPMI 1640/10% human serum. The downstream sample was retrieved. The percentage of ring-stage *Pf*-RBCs in upstream and downstream RBC samples was determined by examination of Giemsa-stained blood films. Experiments were performed on highly synchronized parasites (12–15 h, 15–18 h, 18–21 h and 21–24 h old rings) after incubation at 37°C or 40°C.

Statistical analysis. We calculated *p* values by two-tailed Mann–Whitney rank sum tests comparing the membrane fluctuations and shear moduli values between various test conditions. We used the student-T-test comparing the microspheres filtration results. All of the numbers following the ± sign in the text are standard deviations.

1. Maier AG, R. M. *et al.* Exported proteins required for virulence and rigidity of *Plasmodium falciparum*-infected human erythrocytes. *Cell* **134**, 20–22 (2008).
2. Cooke, B. M. *et al.* Malaria and the red blood cell membrane. *Semin Hematol* **41**, 173–188. (2004).
3. Mills, J. P. *et al.* Nonlinear elastic and viscoelastic deformation of the human red blood cell with optical tweezers. *Mech Chem Biosyst* **1**, 169–180 (2004).
4. Cranston HA, B. C. *et al. Plasmodium falciparum* maturation abolishes physiologic red cell deformability. *Science* **223**, 400–403 (1984).
5. Suresh, S. *et al.* Connections between single-cell biomechanics and human disease states: gastrointestinal cancer and malaria. *Acta Biomater* **1**, 15–30 (2005).
6. Dondorp, A. M. *et al.* Reduced microcirculatory flow in severe falciparum malaria: pathophysiology and electron-microscopic pathology. *Acta Trop* **89**, 309–317 (2004).
7. Nash, G. B. *et al.* Abnormalities in the mechanical properties of red blood cells caused by *Plasmodium falciparum*. *Blood* **74**, 855–861 (1989).
8. Park, Y. *et al.* Refractive index maps and membrane dynamics of human red blood cells parasitized by *Plasmodium falciparum*. *Proc. Natl. Acad. Sci. U.S.A.* **105**, 13730 (2008).
9. Mills, J. P. *et al.* Effect of plasmodial RESA protein on deformability of human red blood cells harboring *Plasmodium falciparum*. *Proc Natl Acad Sci U S A* **104**, 9213–9217 (2007).
10. Aikawa, M. *et al.* Pf155/RESA antigen is localized in dense granules of *Plasmodium falciparum* merozoites. *Experimental Parasitology* **71**, 326–329 (1990).
11. Culvenor, J. G. *et al. Plasmodium falciparum* ring-infected erythrocyte surface antigen is release from merozoite dense granules after erythrocyte invasion. *Infection and Immunity* **59**, 1183–1187 (1991).
12. Foley, M. *et al.* The Ring-infected erythrocyte surface antigen protein of *Plasmodium falciparum* is phosphorylated upon association with the host cell membrane. *Molecular and Biochemical Parasitology.* **38**, 69–76 (1990).

13. Foley, M. *et al.* The ring-infected surface antigen of *Plasmodium falciparum* associates with spectrin in the erythrocyte membrane. *Molecular and Biochemical Parasitology.* **46**, 137–148 (1991).
14. Pei, X. *et al.* The ring-infected erythrocyte surface antigen (RESA) of *Plasmodium falciparum* stabilizes spectrin tetramers and suppresses further invasion. *Blood* **110**, 1036–1042 (2007).
15. Da Silva, E. *et al.* The *Plasmodium falciparum* protein RESA interacts with the erythrocyte cytoskeleton and modifies erythrocyte thermal stability. *Mol Biochem Parasitol* **66**, 59–69 (1994).
16. Silva, M. D. *et al.* A role for the *Plasmodium falciparum* RESA protein in resistance against heat shock demonstrated using gene disruption. *Mol Microbiol* **56**, 990–1003 (2005).
17. Popescu, G. *et al.* Diffraction phase microscopy for quantifying cell structure and dynamics. *Opt. Lett.* **31**, 775–777 (2006).
18. Park, Y. K. *et al.* Diffraction phase and fluorescence microscopy. *Opt. Express* **14**, 8263–8268 (2006).
19. Bow, H. *et al.* A microfabricated deformability-based flow cytometer with application to malaria. *Lab Chip* **11**, 1065–1073 (2011).
20. Deplaine, G. *et al.* The sensing of poorly deformable red blood cells by the human spleen can be mimicked in vitro. *Blood* **117**, e88–95 (2011).
21. Waugh, R. *et al.* Thermoelasticity of red blood cell membrane. *Biophys J* **26**, 115–131 (1979).
22. Minetti, M. *et al.* Spectrin involvement in a 40 degrees C structural transition of the red blood cell membrane. *J Cell Biochem* **30**, 361–370 (1986).
23. Lee, J. C. M. *et al.* Deformation-Enhanced Fluctuations in the Red Cell Skeleton with Theoretical Relations to Elasticity, Connectivity, and Spectrin Unfolding. *Biophys. J.* **81**, 3178–3192 (2001).
24. Srinivasan, P. *et al.* Binding of *Plasmodium* merozoite proteins RON2 and AMA1 triggers commitment to invasion. *Proc Natl Acad Sci U S A* **108**, 13275–13280 (2011).
25. Hossain, M. E. *et al.* The cysteine-rich regions of *Plasmodium falciparum* RON2 bind with host erythrocyte and AMA1 during merozoite invasion. *Parasitol Res* **110**, 1711–1721 (2012).
26. Riglar, D. T. *et al.* Super-resolution dissection of coordinated events during malaria parasite invasion of the human erythrocyte. *Cell Host Microbe* **9**, 9–20 (2011).
27. Li, X. *et al.* A Presenilin-like protease associated with *Plasmodium falciparum* micronemes is involved in erythrocyte invasion. *Mol Biochem Parasitol* **158**, 22–31 (2008).
28. McPherson, R. A. *et al.* Proteolytic digestion of band 3 at an external site alters the erythrocyte membrane organisation and may facilitate malarial invasion. *Mol Biochem Parasitol* **62**, 233–242 (1993).
29. Dluzewski, A. R. *et al.* Red cell membrane protein distribution during malarial invasion. *J Cell Sci* **92 (Pt 4)**, 691–699 (1989).
30. Safeukui, I. *et al.* Retention of *Plasmodium falciparum* ring-infected erythrocytes in the slow, open microcirculation of the human spleen. *Blood* **112**, 2520–2528 (2008).
31. Knuepfer, E. *et al.* Trafficking of the major virulence factor to the surface of transfected P. falciparum-infected erythrocytes. *Blood* **105**, 4078–4087 (2005).
32. Sanyal, S. *et al. Plasmodium falciparum* STEVOR proteins impact erythrocyte mechanical properties. *Blood* **119**, e1–8 (2012).
33. Lambros, C. *et al.* Synchronization of *Plasmodium falciparum* erythrocytic stages in culture. *J.Parasitol.* **65**, 418–420 (1979).

Acknowledgments

The authors thank Peter David for critical reading of this manuscript. M.D-S, MD, and SS acknowledge support for this work from the Interdisciplinary Research Group on Infectious Diseases, which is funded by the Singapore-MIT Alliance for Research and Technology (SMART) Center. YKP was funded by KAIST, KAIST Institute for Optical Science and Technology, National Research Foundation (NRF-2012R1A1A1009082) and the Korean Ministry of Education, Science and Technology (MEST) grant No. 2009-0087691 (BRL). YKP acknowledges support from POSCO TJ Park Fellowship. The authors also acknowledge the support of the SMART BioSyM IRG, the National Institutes of Health (NIH) Grant R01HL094270, and the French Agence Nationale de la Recherche (ANR), under grant MIE (ANR-08-MIE-031) and the support of the National Center for Research Resources of the National Institutes of Health (9P41-EB015871-26A1). GD was funded by grants from the Délégation Générale à l'Armement (fellowship 05 60 00 032), F. Lacoste (Fondation Ackerman - Fondation de France) and the Région Ile de France.

Author Contribution

M.D.-S, and Y.P. designed experiments, performed research, analyzed the data and wrote the paper, S.H., H.B., G.D., C.L. and S.P. performed research and analyzed the data; O.M.-P., S.B., M.S.-F., M.D., J.H. and S.S. designed experiments, analyzed the data, and wrote the paper.

Additional information

Supplementary information accompanies this paper at http://www.nature.com/scientificreports

Competing financial interests: M. Diez-Silva, S. Huang, J. Han, M. Dao, S. Suresh, along with others, have filed two US provisional patents on the microfluidic system. O. Puijalon, G. Deplaine, S. Perrot, along with others, have filed a patent on the microspheres filtration system.

How to cite this article: Diez-Silva, M. *et al.* Pf155/RESA protein influences the dynamic microcirculatory behavior of ring-stage *Plasmodium falciparum* infected red blood cells. *Sci. Rep.* **2**, 614; DOI:10.1038/srep00614 (2012).